A Photocatalytic Approach for the Synthesis of L-Shape Bicyclic NHC Ligands

Tanakorn Kittikool, Kunita Phakdeeyothin, Agustín A Morales, Cécile Barthes, Laure Vendier, Sirilata Yotphan, Sébastien Bontemps, Stéphanie Bastin, Agustí Lledós, Olivier Baslé, et al.

ChemistryEurope
Excellence in Chemistry Research Worldwide

Research Article
doi.org/10.1002/ceur.202300083

www.journal.chemistry-europe.org

A Photocatalytic Approach for the Synthesis of L-Shape Bicyclic NHC Ligands

Tanakorn Kittikool[+],[a, b] Kunita Phakdeeyothin[+],[a, b] Agustín Morales,[a, c] Cécile Barthes,[a] Laure Vendier,[a] Sirilata Yotphan,[b] Sébastien Bontemps,[a] Stéphanie Bastin,[a] Agustí Lledós,*[c] Olivier Baslé,*[a] and Vincent César*[a]

L-shape *N*-Heterocyclic Carbenes (NHCs) based on the imidazo[1,5-*a*]pyridine (ImPy) scaffold have recently gained considerable interest as the true carbene ligand analogues of the popular dialkylbiarylphosphines, better known as Buchwald phosphines. Nevertheless, the substitution pattern of ImPy ligands is still rather limited due to synthetic access issues. We report herein an efficient and versatile visible light photocatalytic strategy to access L-shape bifunctional ImPy ligands laterally-functionalized by a phenol group. Mechanistic investigations supported by density functional theory (DFT) reveal that the excited state of the iridium photocatalyst undergoes either a reductive quenching (SET process) or an energy-transfer quenching (EnT process) depending on the nature of the counterion of the 5-bromoimidazo[1,5-*a*]pyridinium substrate salt. Moreover, the bifunctional character of these new family of L-shape ImPy ligands is demonstrated by the preparation of a gold(I) complex exhibiting a free OH function capable of intermolecular hydrogen bonding. This work highlights the advantage of visible light photocatalysis in the synthesis of advanced NHC ligand structures, a strategy that has not yet been considered despite its potential benefits in terms of versatility, diversity and practicability.

Introduction

Over the last 15 years, the field of visible-light photocatalysis has undergone a significant renaissance and is now recognized as a powerful synthetic tool, which provides new activation modes and bond-forming protocols operating under mild conditions and with good functional group tolerance.[1,2] More recently, *N*-Heterocyclic Carbenes (NHCs), which rank among the most powerful tools in modern chemistry,[3] were successfully implemented in photocatalytic systems. On one hand, as a privileged class of ligands for transition metal complexes,[4] NHCs were incorporated in photoactive organometallic complexes able to efficiently catalyze bond-breaking/forming transformations through visible-light irradiation (Figure 1A).[5] On another hand, the use of NHC as organocatalyst in combination with photoredox catalysis turned out to be a promising strategy for the development of efficient and selective single electron transfer (SET) reactions (Figure 1B).[6] Recently, a benzoxazolium NHC precursor has been used as a stoichiometric alcohol activator for the photoredox-catalyzed C–O bond breaking to generate alkyl radicals, enabling C–C cross-coupling with aryl bromides or carboxylic acids (Figure 1C).[7] Nevertheless, to the best of our knowledge, visible light photocatalysis has not yet been considered in a synthetic approach to directly functionalize NHC precursors,[8] despite the potential benefits in terms of versatility, diversity and practicability.

[a] *T. Kittikool,[+] K. Phakdeeyothin,[+] A. Morales, C. Barthes, Dr. L. Vendier, Dr. S. Bontemps, S. Bastin, Dr. O. Baslé, Dr. V. César*
LCC–CNRS
Université de Toulouse, CNRS, Toulouse, France
E-mail: olivier.basle@lcc-toulouse.fr
vincent.cesar@lcc-toulouse.fr

[b] *T. Kittikool,[+] K. Phakdeeyothin,[+] Prof. S. Yotphan*
Department of Chemistry and Center of Excellence for Innovation in Chemistry
Faculty of Science, Mahidol University
Rama VI Road, Bangkok 10400, Thailand

[c] *A. Morales, Prof. A. Lledós*
Departament de Química
Universitat Autonoma de Barcelona
08193 Cerdanyola del Valles, Catalonia, Spain
E-mail: agusti.lledos@uab.cat

[+] *Authors contributed equally to this work.*

Supporting information for this article is available on the WWW under https://doi.org/10.1002/ceur.202300083

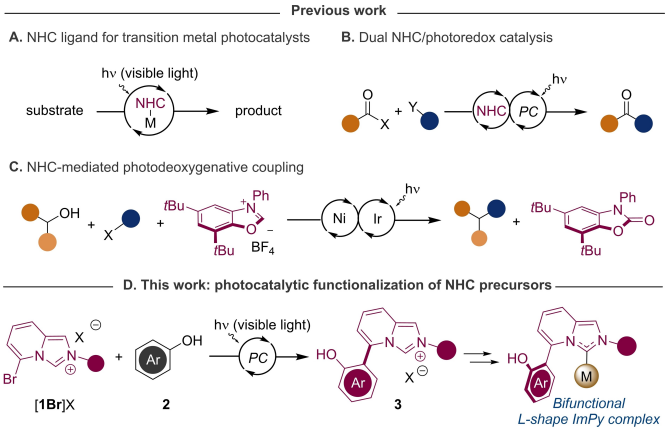

Figure 1. NHCs in photocatalytic reactions: A) As supporting ligands in photocatalytic transition metal complexes; B) In dual NHC/photoredox catalysis; C) NHC precursor as additive for the photocatalytic activation of alcohols; D) As substrates: Photocatalytic direct arylation of NHC precursors.

Research Article
doi.org/10.1002/ceur.202300083

Besides the ubiquitous monocyclic NHC structure, the *N*-fused bicyclic imidazo[1,5-*a*]pyridinylidene scaffold (ImPy), first disclosed in 2005,[9] has gained considerable importance in recent years[10,11] as the structural carbenic mimic of the popular Buchwald dialkylbiarylphosphines.[12] The ImPy platform is particularly effective in transition metal catalysis, including gold(I) catalysis, as the functionalization of the C5 position of the rigid bicyclic heterocycle leads to L-shape NHC ligands, fostering – potentially chiral – stabilizing interactions, or enabling access to bifunctional catalytic systems.[13]

Our group has recently developed various C5-functionalized ImPy ligands through nucleophilic aromatic substitution (SN_{Ar}) of the key 5-bromoimidazo[1,5-*a*]pyridinium bromide [**1Br**]Br by N- or C-nucleophiles such as sodium azide,[14] malonate derivatives,[15] or helicenic fluorenides.[16] Furthermore, since pyridyl radicals generated from halopyridines under photoredox conditions have been identified as key intermediates in carbon-carbon bond formation reactions,[17] we decided to evaluate the potential of halogeno-imidazopyridinium salts, such as [**1Br**]X, as substrates in visible light photocatalysis for the development of an efficient synthetic approach to new L-shape bicyclic NHC ligand precursors bearing additional functional groups, such as a free phenol moiety (Figure 1D).

Results and Discussion

The coupling between 5-bromo-2-mesityl-imidazo[1,5-*a*]pyridinium bromide [**1aBr**]Br and *p*-cresol (**2a**) was chosen as model reaction to determine the optimal reaction conditions to access OH-functionalized L-shape NHC precursor **3a**. We were pleased to observe the coupling product **3a** in 40% yield through irradiation at 456 nm for 16 h in presence of 1 mol% of $Ir(Fppy)_3$ as a photocatalyst (Table 1, entry 1). Screening of the Ir(III) photocatalysts showed that cationic [$Ir(dF(CF_3)ppy)_2(dtbbpy)]PF_6$ and [$[Ir(ppy)_2(dtbbpy)]PF_6$ afforded **3a** in slightly better yields (59% and 50% respectively)(Table 1, entries 2 and 3). Besides, compound **3a** was obtained in only 19% and 8% by using the organic photocatalysts 3DPAFIPN and 4CzIPN (entries 4 and 5). Fortunately, adding 1 equivalent of 2,6-lutidine to quench the released HBr produced during the reaction significantly improved the outcome of the reaction, with a full conversion of [**1aBr**]Br and a 89% yield of **3a** observed (entry 6). **3a** was isolated in 85% yield and was fully characterized by spectroscopic and analytic techniques and its molecular structure was firmly established by an X-Ray diffraction experiment on single crystal (Table 1, insert).[18] Finally, control experiments without light or photocatalysts confirmed the visible-light induced nature and the necessity of a photocatalyst for the coupling reaction (Entries 7 and 8).

With the optimized conditions in hand, we then explored the scope of the arylation reaction by first varying the phenol coupling partner (Table 2). In comparison with the 85% isolated yield obtained for **3a** using cresol, products **3b** and **3c** resulting from the cross-coupling of [**1aBr**]Br with phenol **2b** and mequinol **2c**, respectively, were both isolated with a slightly reduced yield of 77%. On the other hand, the presence of a bulky *tert*-butyl substituent in *para*-position of the phenol did not hamper the reactivity affording the desired product **3d** in high 89% yield. Nevertheless, *para*-halogenated phenol partners such as **2e** and **2f** demonstrated reduced efficiency, almost halving the yields of the desired products. Pleasantly, phenols bearing *ortho*-substituents were suitable partners to produce the arylated products **3g**–**3i** with excellent isolated yields. Similar results were obtained when *meta*-substituted phenols **2j** and **2k** were engaged in the arylation reaction. Interestingly, the coupling reaction with 2-naphtol **2l** demonstrated high efficiency in forming product **3l** with total regioselectivity.

The scope of the arylation reaction was further investigated by changing the nature of the nitrogen substituent of the bromoimidazopyridinium bromide salt [**1Br**]Br (Table 3). When the mesityl group was replaced by a *para*-tolyl in [**1bBr**]Br, the coupling product **3m** with cresol was isolated in 70% yield. Substrate [**1cBr**]Br bearing the bulky 2,6-diisopropylphenyl

Table 1. Optimization studies.[a]

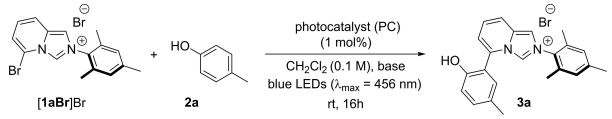

Entry	Photocatalyst (1 mol%)	Base	Conv.	Yield (%)[b]
1	$Ir(Fppy)_3$	–	68	40
2	$[Ir(dF(CF_3)ppy)_2(dtbbpy)]PF_6$	–	95	59
3	$[Ir(ppy)_2(dtbbpy)]PF_6$	–	76	50
4	3DPAFIPN	–	36	19
5	4CzIPN	–	11	8
6	$[Ir(dF(CF_3)ppy)_2(dtbbpy)]PF_6$	2,6-lutidine	>99	89 (85)[c]
7[d]	$[Ir(dF(CF_3)ppy)_2(dtbbpy)]PF_6$	2,6-lutidine	<1	nd[e]
8	none	2,6-lutidine	<1	nd[e]

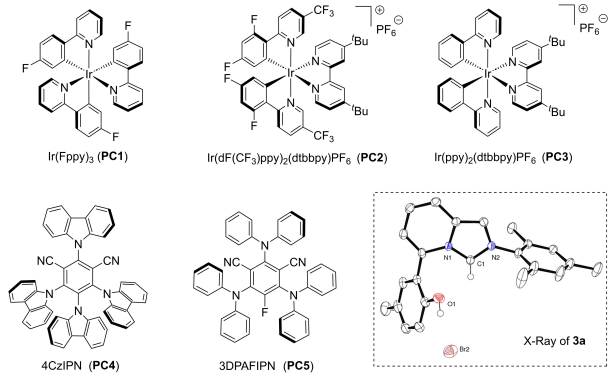

[a]Reaction conditions: [**1aBr**]Br (0.1 mmol), **2a** (0.3 mmol), photocatalyst (1 mol%), 2,6-lutidine (0.1 mmol), CH_2Cl_2 (1 mL), blue LEDs (λ_{max} = 456 nm), Ar, rt, 16 h. [b] Yields were determined by ^1H NMR analysis of the crude reaction mixtures, after HBr (0.1 M) treatment, using 1,3,5-trimethoxybenzene as internal standard. [c] Isolated yield. [d] Performed in the dark. [e] Not detected.

Research Article
doi.org/10.1002/ceur.202300083

Table 2. Scope of phenol partners.[a]

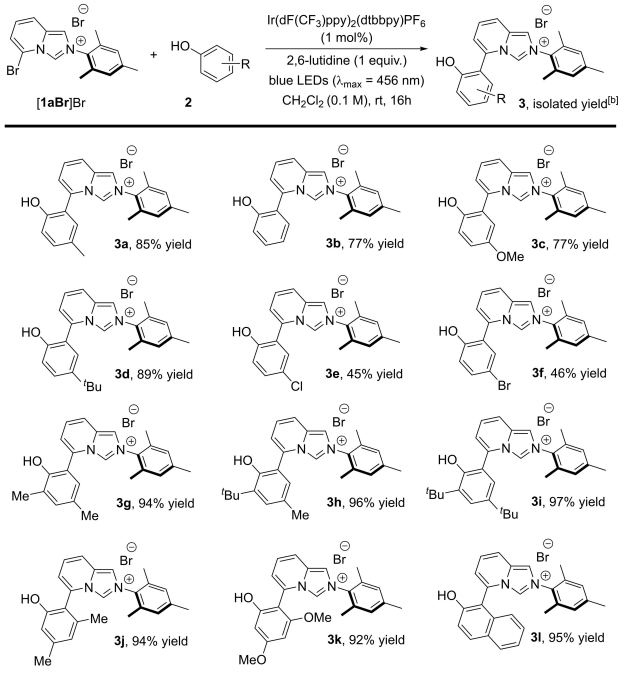

[a] Reaction conditions: [**1aBr**]Br (0.2 mmol), **2** (0.6 mmol), [Ir(dF-(CF_3)ppy)$_2$(dtbbpy)]PF_6 (1 mol%), 2,6-lutidine (0.2 mmol), CH_2Cl_2 (2 mL), blue LEDs (λ_{max} = 456 nm), Ar, rt, 16 h. [b] Yield of isolated product after silica gel chromatography.

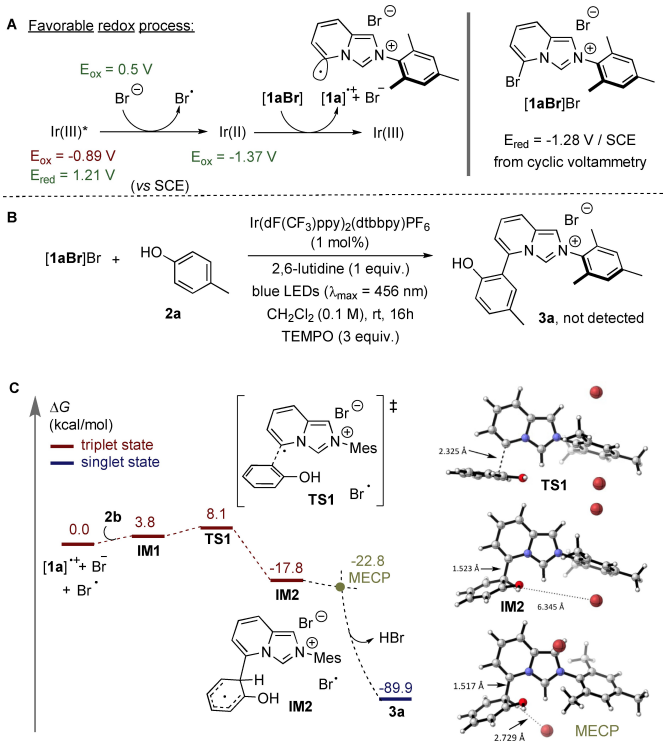

Scheme 1. Mechanistic consideration under photoredox conditions. [A] Favorable redox process with the imidazopyridinium bromide salt [**1aBr**]Br. [B] TEMPO experiment. [C] Computed Gibbs energy profile.

Table 3. Scope of the bromoimidazopyridium bromide salt.[a]

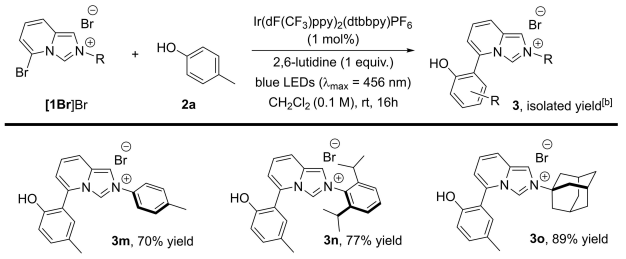

[a] Reaction conditions: [**1Br**]Br (0.2 mmol), **2a** (0.6 mmol), [Ir(dF-(CF_3)ppy)$_2$(dtbbpy)]PF_6 (1 mol%), 2,6-lutidine (0.2 mmol), CH_2Cl_2 (2 mL), blue LEDs (λ_{max} = 456 nm), Ar, rt, 16 h. [b] Yield of isolated product after silica gel chromatography.

group was also amenable affording **3n** in 77% yield. Finally, the scope was not limited to imidazopyridinium salts with aromatic substituents, since excellent 89% isolated yield was obtained for **3o** incorporating an adamantyl group on nitrogen.[19]

To gain insight into the mechanism of the present photocatalytic reaction, a series of experiments were conducted. Upon irradiation, the generated excited state Ir(III)* of the iridium(III) photocatalyst could be oxidatively quenched (E_{ox}[Ir(IV)/Ir(III)*] = −0.89 V/SCE) or reductively quenched (E_{red}[Ir(III)*/Ir(II)] = 1.21 V/SCE) by substrates through a SET process.[20] As the cyclic voltammogram of [**1aBr**]Br showed an irreversible 1e$^-$ reduction peak at −1.28 V/SCE in CH_2Cl_2 (Scheme 1 and Figure S29), the oxidative quenching of Ir(III)* by the [**1aBr**]$^+$ cation appeared unlikely to be operative. Conversely, the reductive quenching of Ir(III)* by the bromide counteranion of [**1aBr**]Br, whose oxidation potential was determined at E = 0.5 V/SCE, can efficiently take place. The resulting highly reducing Ir(II) species (E_{ox}[Ir(III)/Ir(II)] = −1.37 V/SCE) would then be able to engage in single electron transfer with the 5-bromoimidazopyridium ion [**1aBr**]$^+$ inducing the Csp^2-Br bond breaking to produce bromide anion and the corresponding imidazopyridinium radical cation [**1a**]$^{\bullet+}$. The latter would subsequently react with the phenol partner in a stepwise radical process to produce the desired coupling product. Indeed the reaction was suppressed when (2,2,6,6-tetramethylpiperidin-1-yl)oxyl (TEMPO) was added, further suggesting the implication of free radical species in the transformation (Scheme 1B). Thus, DFT calculations were conducted to study the mechanism of the coupling reaction by starting from the set of products {[**1a**]$^{\bullet+}$ + Br$^-$ and Br$^\bullet$} generated from [**1aBr**]Br and photocatalyst as the reference point of the reaction coordinate profile (Scheme 1C). First, association of phenol **2b** leads to intermediate **IM1**, whose energy level is at 3.8 kcal/mol. The latter undergoes a facile C–C bond formation between the radical in [**1a**]$^{\bullet+}$ and the *ortho*-position of the phenol **2b** losing its aromaticity through **TS1** and leading to **IM2**, which was calculated at −17.8 kcal/mol. The computed minimum energy crossing point (MECP) predicts that intersystem crossing (ISC) and hydrogen abstraction by the bromine radical is barrierless to form the coupling product **3**

Research Article
doi.org/10.1002/ceur.202300083

upon rearomatization that is the driving force for the whole process.

With the aim to further understand the role of the bromide counterion in the photoredox process, the efficiency of the coupling reaction was then evaluated using the hexafluorophosphate salt [**1aBr**]PF_6. Surprisingly, and despite its low reduction potential ($E_{red} = -1.36$ V/SCE) preventing it from engaging in SET with the excited state of the iridium catalyst (Figure S30), the catalytic system afforded the desired product in 66% yield after 16 h under blue light irradiation (Figure 2a). Importantly, UV-vis spectroscopic measurements of various combinations of [**1aBr**]PF_6, **2a**, and 2,6-lutidine in CH_2Cl_2, did not reveal the presence of association phenomena with new absorption band in the visible light region, thus ruling out the formation of charge transfer complexes and their potential involvement in the reactivity observed in the absence of bromide ion (Figure 2b).[21] Furthermore, of all the possible reagent combinations, Stern-Volmer experiments demonstrated that only an increasing concentration of [**1aBr**]PF_6 led to a decrease in iridium complex **PC2** luminescence, albeit with a quenching constant almost 50 times lower than that measured in the case of [**1aBr**]Br (Figure 2c).

On the basis of above experimental results, we postulated that, in the absence of bromide anion, an alternative mechanism involving an energy transfer process could be operative. In order to evaluate this hypothesis, the energy of the triplet excited state of [**1aBr**]PF_6 was evaluated by DFT calculations and found to be 56.7 kcal/mol, which is significantly lower than the triplet energy of **PC2** ($E_T = 60.8$ kcal/mol).[22]

Therefore, sensitization of [**1aBr**]PF_6 by **PC2*** is favorable with a thermodynamic driving force (ΔG) of 4.1 kcal/mol. Furthermore, the imidazopyridinium radical ion, product of homoleptic C–Br bond breaking that is predicted to be the key species for the subsequent C–C bond formation reaction (Figure S31), was found to be only 11.6 kcal/mol above this triplet diradical state ^{3}[**1aBr**]PF_6 (Scheme 2). The same calculations were also performed for [**1aBr**]Br, that evidenced a triplet excited state energy of 56.4 kcal mol^{-1} and the product of C–Br bond breaking ([**1a**]$^{\bullet+}$ + Br$^{\bullet}$ + Br$^-$) only 3.4 kcal mol^{-1} above the corresponding triplet ^{3}[**1aBr**]Br excited state. It was also discovered that the reaction can occur in the absence of photocatalyst through the direct excitation of [**1aBr**]Br or [**1aBr**]PF_6 under UV LEDs ($\lambda_{max} = 365$ nm) irradiation (Scheme 3). The better reactivity of the bromide salt under UV irradiation could be justified by its longer wavelength absorbance compare to [**1aBr**]PF_6 and a slight increased overlap with the emission spectrum of the 365 nm LEDs (Figure S22). These results, along with additional time-dependent DFT calculations (Figures S32, S35 and Table S1), further corroborate the assumption of the existence of an alternative mechanism with the implication of excited state intermediates.

Based on all the above experimental and theoretical studies, a proposed general mechanism is shown in Scheme 4. First, absorbance of a visible light photon by the Ir(III) complex generates the reactive triplet excited state Ir(III)* species. Then, two possible quenching events may occur. On one hand, [**1aBr**]X (X = Br, PF_6) may engage in an energy transfer process with Ir(III)* to generate the triplet excited state ^{3}[**1aBr**]X, which would undergo homoleptic C–Br bond breaking to produce bromine radical (Br$^{\bullet}$) and the imidazopyridinium radical ion

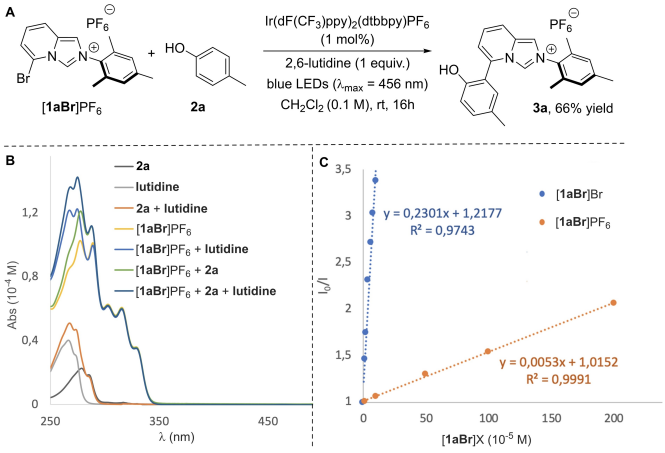

Figure 2. [A] Reactivity of [**1aBr**]PF_6 under standard conditions. [B] UV-vis spectroscopic measurements (C = 10^{-4} M). [C] Stern-Volmer quenching plot of **PC2** by [**1aBr**]Br and [**1aBr**]PF_6 in CH_2Cl_2.

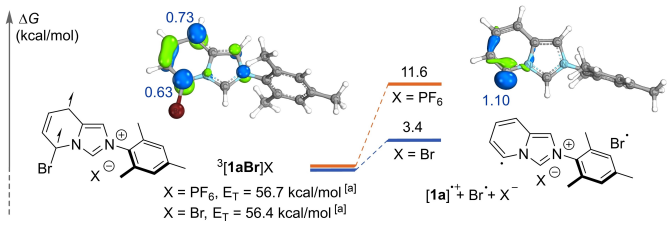

Scheme 2. Energy change from calculated triplet excited state ^{3}[**1aBr**]Br and ^{3}[**1aBr**]PF_6 to products of homoleptic carbon-bromine bond cleavage. DFT-calculated SOMO of ^{3}[**1aBr**] and of [**1a**]$^{\bullet+}$, and Mulliken spin density (blue values).

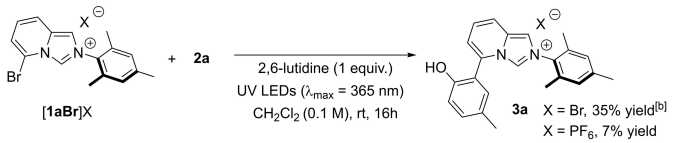

Scheme 3. Direct excitation under UV light irradiation. Yields were determined by ^{1}H NMR analysis of the crude reaction mixtures, after HBr (0.1 M) treatment, using 1,3,5-trimethoxybenzene as internal standard.

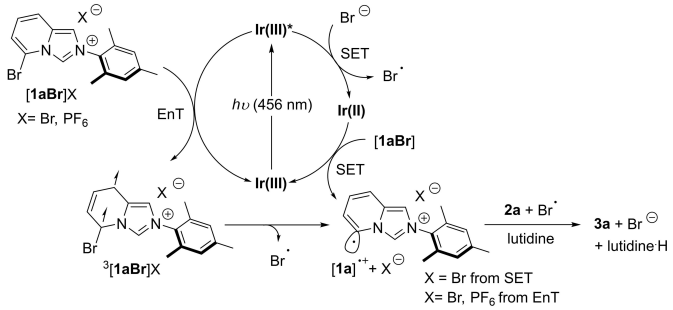

Scheme 4. Proposed overall mechanism involving either and EnT process (left) or a SET process (right).

Research Article
doi.org/10.1002/ceur.202300083

[**1 a**]$^{\bullet+}$. On the other hand, the alternative pathway involves first reductive quenching of Ir(III)* by a bromide ion to form bromine radical and Ir(II), which is able to engage in SET process to reduce [**1aBr**]$^{+}$ and form bromide ion along with the key imidazopyridinium radical cation [**1 a**]$^{\bullet+}$. In both cases, the subsequent C–C bond forming reaction between [**1 a**]$^{\bullet+}$, **2 a** and Br$^{\bullet}$ in the presence of lutidine produces the desired cross-coupling product **3 a** and lutidinium bromide. While the SET process is favored with [**1aBr**]Br as starting material, the EnT mechanism is necessarily operative at the early stage of the reaction with [**1aBr**]PF_6 due to the absence of bromide ion. Nevertheless, the stoichiometric release of bromide ion during the formation of **3 a** will induce a switch towards the more kinetically favored SET mechanism pathway.

Finally, to demonstrate that OH-functionalized L-shape NHC can actually play the role of ancillary ligand for transition metals, the synthesis of a NHC-gold(I) complex was then undertaken (Scheme 5). The representative **3 g** was thus deprotonated by two equivalents of KHMDS in THF at −78 °C to give the corresponding free anionic NHC, which was trapped by chloro(tetrahydrothiophene)gold(I). A last *in situ* reprotonation of the phenolate moiety using HBr led to the isolation of the desired NHC-Au(I)Br complex **4 g** in 45 % isolated yield. The complex was fully characterized by spectroscopic and analytic techniques and its molecular structure was further established by an X-Ray diffraction experiment on single crystal grown in acetone. As expected, the ImPy ligand displays a L-shape arrangement around the gold(I) center. Noteworthy, the free phenol OH group in the second coordination sphere is engaged in a hydrogen bonding interaction with the oxygen atom of an acetone molecule.

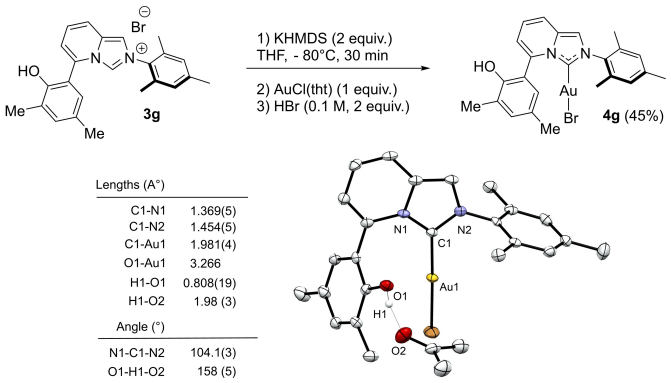

Scheme 5. Synthesis of Au(I) complex **4 g** and its structure determined by X-ray diffraction analysis. All hydrogen atoms except the OH one have been omitted for clarity. Selected bond lengths and distances (Å) and angles (deg).

Conclusions

In summary, we developed an efficient and straightforward visible-light photocatalytic approach towards the synthesis of a novel class of OH-functionalized L-shape NHC ligands based on the ImPy scaffold. The key intermediate was shown to be an imidazopyridinium radical generated from the carbon-bromine bond breaking of 5-bromoimidazo[1,5-*a*]pyridinium salts, which undergoes a radical addition on the phenol derivatives. Noteworthy, the photocatalytic protocol was shown to proceed through two parallel quenching processes, based on either single electron transfer (SET) or energy transfer (EnT). Through this first example, it has been demonstrated that visible-light photocatalytic functionalization of NHC precursors is a promising synthetic tool to access novel carbenic scaffolds, with unprecedented properties, functionalities or spatial arrangement. Extension of this methodology to the design of original (chiral) NHC ligands as well as their applications in asymmetric organometallic catalysis are currently underway in our laboratories.

Acknowledgements

We acknowledge the Centre National de la Recherche Scientifique (CNRS) and the Science Achievement Scholarship of Thailand (to TK and KP). This work was supported by the European Union's Horizon 2020 research and innovation program under the Marie Skłodowska-Curie grant agreement No. 860322 (to AM) and the Agence Nationale de la Recherche (ANR "TCDCat").

Conflict of Interests

The authors declare no conflict of interest.

Data Availability Statement

The data that support the findings of this study are available from the corresponding author upon reasonable request.

Keywords: *N*-heterocyclic carbenes · Photocatalysis · C–C coupling · Mechanistic studies · DFT calculations

[1] C. R. J. Stephenson, T. P. Yoon, D. W. C. MacMillan *Visible light photocatalysis in organic chemistry*, 1st ed. (Eds.: C. R. J. Stephenson, T. P. Yoon, D. W. C. MacMillan), Wiley-VCH, Weinheim, Germany, **2018**.
[2] a) K. P. S. Cheung, S. Sarkar, V. Gevorgyan, *Chem. Rev.* **2022**, *122*, 1543; b) F. Glaser, O. S. Wenger, *Coord. Chem. Rev.* **2020**, *405*, 213129; c) L. Marzo, S. K. Pagire, O. Reiser, B. König, *Angew. Chem. Int. Ed.* **2018**, ***57***, 10034; d) M. H. Shaw, J. Twilton, D. W. C. MacMillan, *J. Org. Chem.* **2016**, *81*, 6898.
[3] M. N. Hopkinson, C. Richter, M. Schedler, F. Glorius, *Nature* **2014**, *510*, 485.
[4] a) Q. Zhao, G. Meng, S. P. Nolan, M. Szostak, *Chem. Rev.* **2020**, *120*, 1981; b) J. Thongpaen, R. Manguin, O. Baslé, *Angew. Chem. Int. Ed.* **2020**, *59*, 10242; c) C. Romain, S. Bellemin-Laponnaz, S. Dagorne, *Coord. Chem. Rev.* **2020**, *422*, 213411; d) E. Peris, *Chem. Rev.* **2018**, *118*, 9988.
[5] a) E. M. Poland, C. C. Ho, *Appl. Organomet. Chem.* **2022**, e6746; b) H. Amouri, *Chem. Rev.* **2023**, *123*, 230.
[6] a) K. Liu, M. Schwenzer, A. Studer, *ACS Catal.* **2022**, *12*, 11984; b) Q. Liu, X.-Y. Chen, *Org. Chem. Front.* **2020**, *7*, 2082.
[7] a) Z. Dong, D. W. C. MacMillan, *Nature* **2021**, *598*, 451; b) H. A. Sakai, D. W. C. MacMillan, *J. Am. Chem. Soc.* **2022**, *144*, 6185; c) W. P. Carson Ii,

Research Article
doi.org/10.1002/ceur.202300083

P. J. Sarver, N. S. Goudy, D. W. C. MacMillan, *J. Am. Chem. Soc.* **2023**, *145*, 20767.

[8] For a review on the synthesis of NHC precursors, see: L. Benhamou, E. Chardon, G. Lavigne, S. Bellemin-Laponnaz, V. César, *Chem. Rev.* **2011**, *111*, 2705.

[9] a) M. Alcarazo, S. J. Roseblade, A. R. Cowley, R. Fernández, J. M. Brown, J. M. Lassaletta, *J. Am. Chem. Soc.* **2005**, *127*, 3290; b) C. Burstein, C. W. Lehmann, F. Glorius, *Tetrahedron* **2005**, *61*, 6207.

[10] For reviews, see: a) P. Teixeira, S. Bastin, V. César, *Isr. J. Chem.* **2022**, *63*, e202200051; b) N. U. D. Reshi, J. K. Bera, *Coord. Chem. Rev.* **2020**, *422*, 213334; c) J. Iglesias-Siguenza, C. Izquierdo, E. Diez, R. Fernandez, J. M. Lassaletta, *Dalton Trans.* **2016**, *45*, 10113.

[11] For relevant examples of 5-aryl-ImPy ligands, see: a) T. Zhou, P. Gao, E. Bisz, B. Dziuk, R. Lalancette, R. Szostak, M. Szostak, *Catal. Sci. Technol.* **2022**, *12*, 6581; b) M. Kashihara, R.-L. Zhong, K. Semba, S. Sakaki, Y. Nakao, *Chem. Commun.* **2019**, *55*, 9291; c) Y. Kim, Y. Kim, M. Y. Hur, E. Lee, *J. Organomet. Chem.* **2016**, *820*, 1; d) F. Grande-Carmona, J. Iglesias-Sigüenza, E. Álvarez, E. Díez, R. Fernández, J. M. Lassaletta, *Organometallics* **2015**, *34*, 5073; e) M. Espina, I. Rivilla, A. Conde, M. M. Díaz-Requejo, P. J. Pérez, E. Álvarez, R. Fernández, J. M. Lassaletta, *Organometallics* **2015**, *34*, 1328; f) J. Francos, F. Grande-Carmona, H. Faustino, J. Iglesias-Sigüenza, E. Díez, I. Alonso, R. Fernández, J. M. Lassaletta, F. López, J. L. Mascareñas, *J. Am. Chem. Soc.* **2012**, *134*, 14322.

[12] B. T. Ingoglia, C. C. Wagen, S. L. Buchwald, *Tetrahedron* **2019**, *75*, 4199.

[13] Recent examples: a) P. Gao, J. Xu, T. Zhou, Y. Liu, E. Bisz, B. Dziuk, R. Lalancette, R. Szostak, D. Zhang, M. Szostak, *Angew. Chem. Int. Ed.* **2023**, *62*, e202218427; b) S. C. Scott, J. A. Cadge, G. K. Boden, J. F. Bower, C. A. Russell, *Angew. Chem. Int. Ed.* **2023**, *62*, e202301526; c) V. K. Rawat, K. Higashida, M. Sawamura, *ACS Catal.* **2022**, *12*, 8325; d) R. Pedrazzani, A. Pintus, R. De Ventura, M. Marchini, P. Ceroni, C. Silva López, M. Monari, M. Bandini, *ACS Org. Inorg. Au* **2022**, *2*, 229; e) J.-Q. Zhang, Y. Liu, X.-W. Wang, L. Zhang, *Organometallics* **2019**, *38*, 3931.

[14] K. Azouzi, C. Duhayon, I. Benaissa, N. Lugan, Y. Canac, S. Bastin, V. César, *Organometallics* **2018**, *37*, 4726.

[15] a) Y. Tang, I. Benaissa, M. Huynh, L. Vendier, N. Lugan, S. Bastin, P. Belmont, V. César, V. Michelet, *Angew. Chem. Int. Ed.* **2019**, *58*, 7977; b) I. Benaissa, L. Pallova, M.-E. Morantin, T. Lafitte, M. Huynh, C. Barthes, L. Vendier, N. Lugan, S. Bastin, V. César, *Chem. Eur. J.* **2019**, *25*, 13030.

[16] L. Pallova, L. Abella, M. Jean, N. Vanthuyne, C. Barthes, L. Vendier, J. Autschbach, J. Crassous, S. Bastin, V. César, *Chem. Eur. J.* **2022**, *28*, e202200166.

[17] a) R. A. Aycock, H. Wang, N. T. Jui, *Chem. Sci.* **2017**, *8*, 3121; b) A. J. Boyington, M.-L. Y. Riu, N. T. Jui, *J. Am. Chem. Soc.* **2017**, *139*, 6582; c) C. P. Seath, D. B. Vogt, Z. Xu, A. J. Boyington, N. T. Jui, *J. Am. Chem. Soc.* **2018**, *140*, 15525; d) S.-Y. Guo, F. Yang, T.-T. Song, Y.-Q. Guan, X.-T. Min, D.-W. Ji, Y.-C. Hu, Q.-A. Chen, *Nat. Commun.* **2021**, *12*, 6538; e) H.-H. Li, S. Li, J. K. Cheng, S.-H. Xiang, B. Tan, *Chem. Commun.* **2022**, *58*, 4392.

[18] CCDC-2302846-2302849 contain the supplementary crystallographic data for this paper. These data are provided free of charge by the joint Cambridge crystallographic Data Centre and Fachinformationszentrum Karlsruhe Access Structures service *via* www.ccdc.cam.ac.uk/structures.

[19] Due to the synthetic access towards the 5-bromoimidazo[1,5 a)]pyridinium bromide [**1Br**]Br, the *N*-adamantyl [**1dBr**]Br was the only *N*-alkyl derivative tested in this study.

[20] J. Ma, S. Chen, P. Bellotti, R. Guo, F. Schäfer, A. Heusler, X. Zhang, C. Daniliuc, M. K. Brown, K. N. Houk, F. Glorius, *Science* **2021**, *371*, 1338.

[21] The visible-light, photocatalyst-free coupling between aryl bromides and phenols in basic media through intermediacy of an EDA complex was recently reported: D.-L. Zhu, S. Jiang, D. J. Young, Q. Wu, H.-Y. Li, H.-X. Li, *Chem. Commun.* **2022**, *58*, 3637.

[22] F. Strieth-Kalthoff, M. J. James, M. Teders, L. Pitzer, F. Glorius, *Chem. Soc. Rev.* **2018**, *47*, 7190.

Version of record online: February 13, 2024